Journal of Applied Mechanics and Technical Physics, Vol. 51, No. 2, pp. 211–217, 2010

CONTROL OF THE VORTEX FLOW AROUND A CONE WITH A SPARK DISCHARGE

A. A. Maslov,[1,2] A. A. Sidorenko,[1] A. D. Budovskiy,[1] B. Yu. Zanin,[1] V. V. Kozlov,[1,2] B. V. Postnikov,[1] and V. P. Fomichev[1]

UDC 532.526.5

A subsonic flow around a cone mounted at an angle of attack is considered. A separated flow is formed on the cone with formation of a pair of large-scale streamwise vortices arranged symmetrically or asymmetrically, depending on flow parameters. The possibility of controlling the vortex flow by means of an electric discharge is studied in experiments. It is demonstrated that the use of an electric discharge makes it possible both to transform an asymmetric flow to symmetric and to generate directed asymmetry. Controlling the flow asymmetry, in turn, allows the side force direction to be controlled.

Key words: *flow around a cone, subsonic flow, separated flow, vortex flow control, electric discharge.*

Introduction. This work continues our research of the possibility of controlling vortex structures formed in the flow around bodies of revolution at an angle of attack. Flow control is ensured by an electric discharge.

A specific feature of the flow around axisymmetric bodies at high angles of attack is the formation of a conical vortex flow with a dominating pair of primary vortices (Fig. 1). The arising vortices induce a reduced pressure region on the leeward side of the body, thus, promoting the emergence of the lift force whose vector may have either a constant or a variable direction, depending on the vortex flow character. As a symmetric vortex configuration becomes asymmetric (see Fig. 1), there appears a side load, which is the projection of the lift force vector onto the horizontal plane. Moreover, vortex asymmetry may become unsteady, which generates a side force with a variable sign.

The transformation of the symmetric flow to asymmetric is explained in [1–3] by the loss of stability of the vortex flow on exceeding the critical ratio of the angle of attack α to the cone half-angle θ. In this case, a small perturbation can initiate a spontaneous transformation of a symmetric vortex configuration to an asymmetric configuration. The initial perturbation can be induced by minor asymmetry of the nose part, roughness, or external flow nonuniformity. In addition, the instant of the flow asymmetry emergence depends on the state of the boundary layer in the pre-separation flow region [4, 5].

In contrast to mechanical [6–8] or jet [9] systems, the control systems based on an electric discharge can adapt to rapidly changing flight parameters. Simplicity of realization, insignificant mass, and absence of violation of the body shape and additional drag allow these systems to be used in real flying vehicles. Moreover, this method does not involve any mechanical or pneumatic devices. For this reason, electric-discharge actuators can be easily scaled and integrated into the overall control system of the flying vehicle. By means of rapid changes in the discharge frequency and power, one can easily and rapidly control the action intensity in flow control systems with feedback. An advantage of such systems is the possibility of using them at high g-loads, because they do not contain moving control surfaces.

[1]Khristianovich Institute of Theoretical and Applied Mechanics, Siberian Division, Russian Academy of Sciences, Novosibirsk 630090; maslov@itam.nsc.ru; sindr@itam.nsc.ru; budovsky@itam.nsc.ru; zanin@itam.nsc.ru; kozlov@itam.nsc.ru; boris@itam.nsc.ru; fomichev@itam.nsc.ru. [2]Novosibirsk State University, Novosibirsk 630090.
Translated from Prikladnaya Mekhanika i Tekhnicheskaya Fizika, Vol. 51, No. 2, pp. 81–89, March–April, 2010. Original article submitted April 8, 2009.

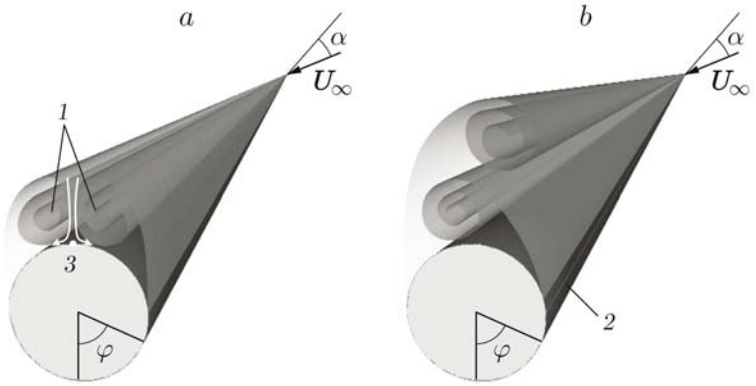

Fig. 1. Flow around an axisymmetric cone at a high angle of attack with symmetric (a) and asymmetric (b) vortex configurations: 1) primary vortex; 2) separation line; 3) saddle point.

The results of the first experiments with the arc discharge were described in [10, 11]. The study of the discharge effect on the air flow near the surface, which was performed on a model setup, showed that the arc discharge generates an intense heat release area and makes the flow streamlines move away from the wall [10]. These results agree with observations described in [12]. Thus, the flow control method implied from the very beginning that the electric discharge can change the positions of the flow separation lines on both sides of the cone. In this case, the discharge can be considered as a source of artificial periodic oscillations, or as a local heat source, or as a stationary step on the cone surface. In all variations, the role of the discharge is to introduce additional perturbations into the flow and to shift the separation region upstream with respect to the crossflow saddle point (see Fig. 1). As a result, the vortices are shifted to a larger distance from the surface, and the distance between the vortex centers increases. The crossflow saddle point moves closer to the model surface, which ensures a more stable state of the flow, preventing the emergence of asymmetry.

The data obtained previously show that the electric discharge can make the flow symmetric, but also can generate directed asymmetry [10]. It is shown that the electric discharge induces the same changes in the vortex pattern as the linear vortex generators in the form of ribs mounted near the primary separation line and designed to fix the flow separation line on the sharp edges of these ribs. The results of studying similar steps were described, for instance, in [13]. The efficiency of vortex generators increases with increasing their length. It was demonstrated, however, that even small steps can ensure a symmetric flow if these steps are located near the model tip. In this case, the vortex cores are located closer to each other, but the flow remains symmetric. This result agrees with the experimental results of [9, 14], where it was shown that even a small action applied near the model tip can alter the flow pattern in the downstream direction. The experiments showed that the discharge power necessary for effective control also decreases as the discharge point approaches the model tip, i.e., the region of vortex origination [10]. For this reason, the vortex flow on a sharp cone with the minimum distance between the model tip and the first discharge gap being 15% of the model length could not be effectively controlled. The desired result could be achieved only with a blunted cone [10], which made it possible to reduce the distance between the region of vortex incipience to the discharge gap to 6% of the body length.

The experiments revealed a number of drawbacks in the previously used control system [10]. The main drawback was the fact that the power circuit of the discharges did not allow smooth variations of the powers of the left and right discharges independent of each other. In addition, the discharge structure did not allow variations of the action length, which was limited by the distance between two neighboring electrodes (10 mm). A small lifetime of the discharger due to erosion of the electrodes and dielectric insert stimulated the search for new possibilities of solving this problem.

Thus, the main objective of this work is to study the efficiency of the vortex structure control method with a possibility of reducing the energy input into the discharge. This study involve investigations of the physical features of the three-dimensional flow near the model tip and optimization of the electric circuit of power supply to the dischargers. As the flow around a model with a sharp tip is a simpler model case, as compared to the blunted cone, and is free from unsteadiness induced by flow separation on the model tip, the study was performed on a sharp

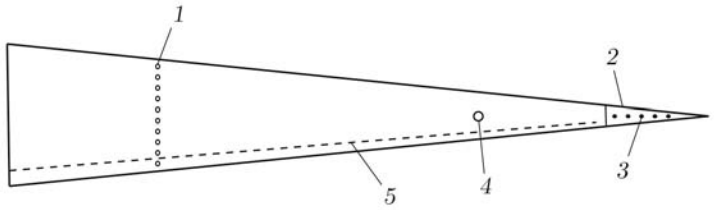

Fig. 2. Sketch of the experimental model: 1) pressure taps; 2) replaceable tip; 3) electrodes; 4) orifice for smoke injection; 5) tripping device.

cone model. For this reason, it was necessary to change the discharger structure to ensure a possibility of initiating the discharge at the minimum distance from the tip and varying the length of the energy-supply zone.

1. Experimental Equipment. The experiments were performed in a T-324 low-turbulence subsonic wind tunnel based at the Khristianovich Institute of Theoretical and Applied Mechanics of the Siberian Division of the Russian Academy of Sciences. The wind tunnel with a square test section ($1 \times 1 \times 4$ m) ensures an extremely uniform flow (the level of turbulence is Tu = 0.04%). The experiments were performed in the range of velocities from 5 to 20 m/sec.

The experimental model was an axisymmetric cone with a sharp tip; the cone length was 1 m, and the apex half-angle was $\theta = 5^\circ$ (Fig. 2). The model was mounted in the test section on a strut, which made it possible to vary the angle of attack in the range $\alpha = 0$–45°.

To monitor the state of the vortex configuration in the course of the experiments, smoke visualization of the flow by the laser sheet technique was performed, and the pressure on the model surface was measured. The laser sheet plane was aligned perpendicular to the model axis. Smoke was inserted into the flow through orifices on the cone surface and was fed through pipelines placed inside the model. The orifices were located opposite to each other at an angle $\varphi = \pm 90^\circ$ with respect to the flow reattachment line (see Fig. 2). The flow rate of air through these orifices was chosen to avoid disturbing the vortex flow. Such an approach ensured a high concentration of tracers in the vortex, which improved the quality of the flow patterns obtained. The trajectories of the illuminated particles in the laser sheet plane were recorded by a video camera located on a strut downstream from the base section of the model.

The surface pressure on the model was measured at 20 points uniformly distributed over the circumference in the cross section $x = 0.576$ m with respect to the model tip (see Fig. 2). First, the measurements were performed by strain-gauge transducers, which were connected by pneumatic pipelines with the pressure taps on the cone. The signals were digitized with an Agilent 34970A data acquisition system. This method ensures high accuracy of measurements, but insufficient noise immunity. As a certain level of power is reached, the electric interferences generated by the discharge become much greater than the valid signal. The emergence of these interferences is caused by the periodic character of the signal feeding the spark discharge (see Sec. 2). To solve this problem, we used the classical method of pressure measurements by a multichannel liquid manometer. The manometer readings were recorded by a digital camera. The resultant photographs were analyzed by a special program that calculated the values of the pressure coefficient C_p.

2. Method of Discharge Generation. Electric Circuit. To protect the surface from erosion inevitable in arc-discharge experiments, the model portion subjected to the high-temperature discharge was made of jade. This part of the model is the replaceable tip (see Fig. 2) with flush-mounted electrodes. This structure allowed us to generate a spark discharge on the surface, which was assumed to be used in this series of experiments. Two arrays of the electrodes were aligned opposite to each other near the lines of the primary flow separation along the cone generatrices at an angle $\varphi = \pm 90^\circ$ with respect to the flow reattachment line. Each array included 12 electrodes with the distance between the neighboring electrodes $h = 5$ mm. The distance from the model tip to the first electrode was 40 mm. A new electric power circuit was specially developed and assembled to perform experiments with a line spark discharge (Fig. 3).

The signal from the generator passed to a thyratron Th, which ensured the discharge of the capacitor C_0 charged through a ballast resistance $R = 41.5$ kΩ. The capacity C_0 was charged by a high-voltage (up to 10 kV) source of rectified voltage of power-supply frequency. With a step-up pulse transformer T, the discharge array

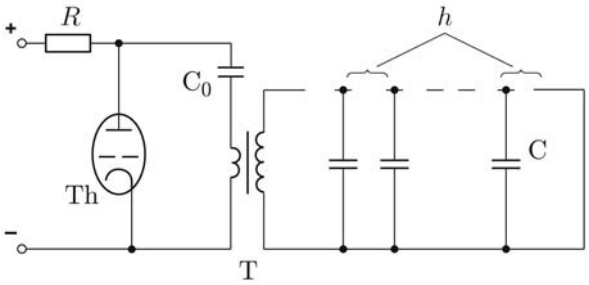

Fig. 3. Electric power circuit for the spark discharge.

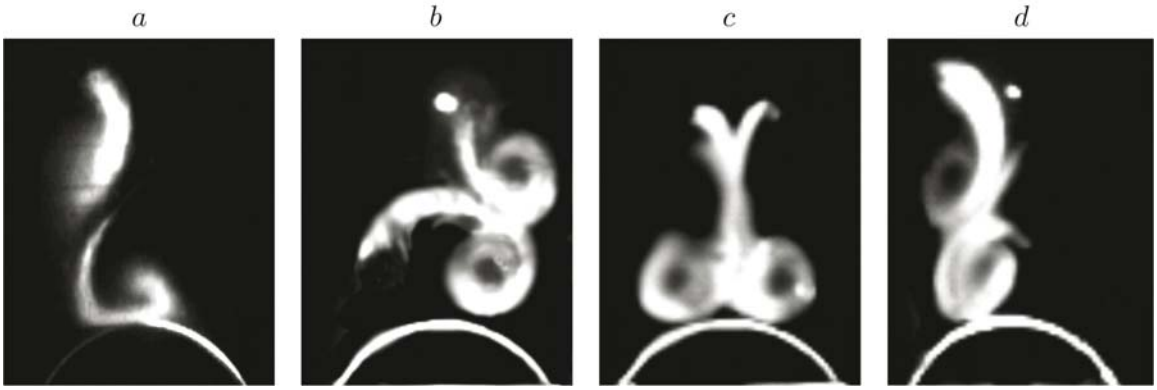

Fig. 4. Evolution of the vortex structure with variations of the discharge powers on two sides of the cone (U_∞ = 10 m/sec and $\alpha = 22.5°$): (a) $W_1 = 0$ and $W_2 = 0$; (b) $W_1 = 44.8$ W and $W_2 = 11.2$ W; (c) $W_1 = 44.8$ W and $W_2 = 44.8$ W; (d) $W_1 = 11.2$ W and $W_2 = 44.8$ W.

capacitors C were charged to 20 kV. The pulse repetition frequency in this array was determined by the master clock frequency of the generator. A thyratron with an operation frequency up to 1 kHz was used in our experiments. The power-supply circuit (see Fig. 3) was duplicated to ensure independent power supply to each discharge array. This power-supply circuit made it possible to adjust the operation parameters of the dischargers independent of each other. Depending on the number of electrodes used, the length of the energy input region could be 5 to 60 mm.

3. Experimental Results. We studied the flow around a cone with separation of the turbulent boundary layer, which allowed us to avoid problems caused by different positions of the laminar–turbulent transition and to ensure equivalent conditions of boundary-layer separation over the entire model length. In addition, it is turbulent separation that occurs in such flows around real flying vehicles. For artificial tripping of the boundary layer, sandpaper strips were glued onto the model along the cone generatrices at an angle $\varphi = \pm 35°$ with respect to the flow reattachment line. The sandpaper strips were located at a distance of 120 mm from the model tip; their application in the nose region is ineffective because of low local Reynolds numbers. The state of the boundary layer was monitored by a hot-wire anemometer. Preliminary experiments showed that turbulent separation ensures the location of the primary separation line downstream of the discharge zone, which allows the location of this line to be deliberately changed.

The study was performed in a flow with a free-stream velocity U_∞ = 10 m/sec in the range of the angles of attack α = 15–30°. The choice of this free-stream velocity was conditioned by the necessity of providing a comparatively high smoke concentration for flow visualization with a low velocity of smoke blowing. The power of the spark discharge in each channel was varied in the experiments in the range from 5.5 W to the maximum value of the order of 50 W. With the use of eight electrodes in each array, the total discharge length was 40 mm.

The action of the discharge on the vortex configuration can be estimated on the basis of the smoke visualization results. Figure 4 shows the typical configurations of the vortex flow under the action of the electric discharge.

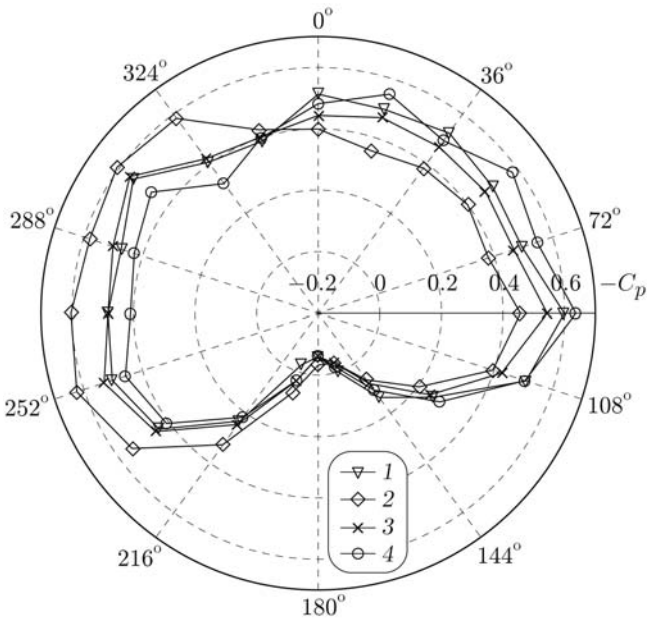

Fig. 5. Distribution of the pressure coefficient for different discharge powers on two sides of the cone ($U_\infty = 10$ m/sec and $\alpha = 22.5°$): 1) $W_1 = 0$ and $W_2 = 0$; 2) $W_1 = 44.8$ W and $W_2 = 11.2$ W; 3) $W_1 = 44.8$ W and $W_2 = 44.8$ W; 4) $W_1 = 11.2$ W and $W_2 = 44.8$ W.

According to [1, 3], the emergence of asymmetry in the flow pattern should be expected at $\alpha/\theta > 3.5$. The results shown in Fig. 4 were obtained at $\alpha/\theta = 4.5$, which ensured the initial asymmetry of the vortex pattern (see Fig. 4a). In the case considered, the right-hand discharge was first initiated, and its power W_1 was gradually increased from 5.5 W to 44.8 W. After that, the power of the left-hand discharge W_2 was increased in the same manner, and then the power of the right-hand discharge was gradually decreased. It is seen that the initially observed asymmetry on the left (in Fig. 4a, the left-hand vortex is higher than the right-hand vortex) was transformed to the asymmetry on the right (see Fig. 4b) with a gradual increase in the right-hand discharge power to the maximum value. A smooth increase in the left-hand discharge power gradually made the vortex pattern symmetric (see Fig. 4c). A smooth decrease in the right-hand discharge power and retaining the maximum power of the left-hand discharge returned the vortex pattern to the initial state (see Fig. 4d). It should be noted that the results shown here correspond to individual frames of one run and describe the behavior of vortices typical for all subsequent runs in this series of experiments.

Figure 5 shows the distributions of the pressure coefficient $C_p = (P - P_n)/q_\infty$ over the model surface in the control section (P is the free-stream static pressure, P_n is the pressure on the model surface, and q_∞ is the dynamic pressure based on free-stream parameters). The distributions of C_p plotted in Fig. 5 correspond to the results in Fig. 4. It is seen that the emergence of flow asymmetry leads to an increase in pressure on one side of the cone and to a decrease in pressure on the other side of the cone. The increase in pressure is caused by the vortex moving away from the model surface, and the decrease in pressure is caused by the approaching vortex.

Based on the surface pressure distributions, we calculated the local coefficients of the side force $C_z = \frac{1}{d}\oint\limits_l C_{p_z}\, dl$ in the control section (d is the local diameter, l is the local circumference length, and C_{p_z} is the projection of the pressure force vector onto the horizontal plane).

The dependence $C_z(T)$ in Fig. 6 corresponds to the results in Fig. 5 with the only difference that Fig. 6 includes the intermediate values of the discharge powers. Positive values of C_z in Fig. 6 refer to the situation with the right-hand vortex located higher than the left-hand vortex (asymmetry on the right), and negative values of C_z correspond to asymmetry on the left.

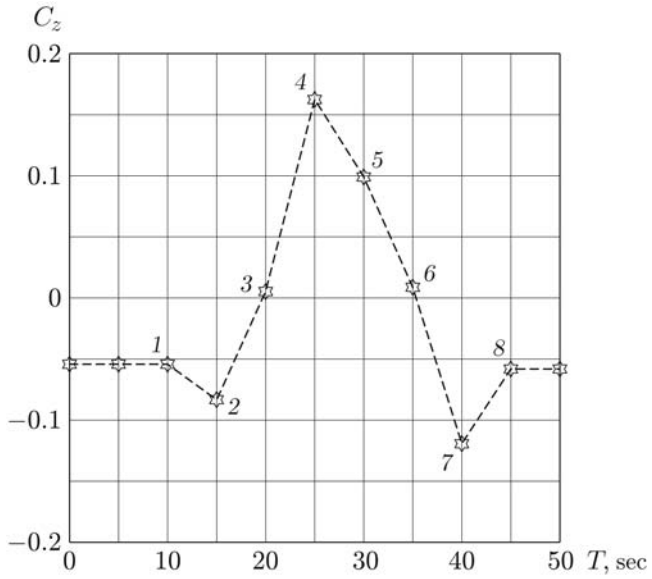

Fig. 6. Time evolution of the side force in a vortex flow subjected to electric discharges (U_∞ = 10 m/sec and $\alpha = 22.5°$): 1) $W_1 = 0$ and $W_2 = 0$; 2) $W_1 = 11.2$ W and $W_2 = 0$; 3) $W_1 = 44.8$ W and $W_2 = 0$; 4) $W_1 = 44.8$ W and $W_2 = 11.2$ W; 5) $W_1 = 44.8$ W and $W_2 = 25.2$ W; 6) $W_1 = 44.8$ W and $W_2 = 44.8$ W; 7) $W_1 = 11.2$ W and $W_2 = 44.8$ W; 8) $W_1 = 0$ and $W_2 = 0$.

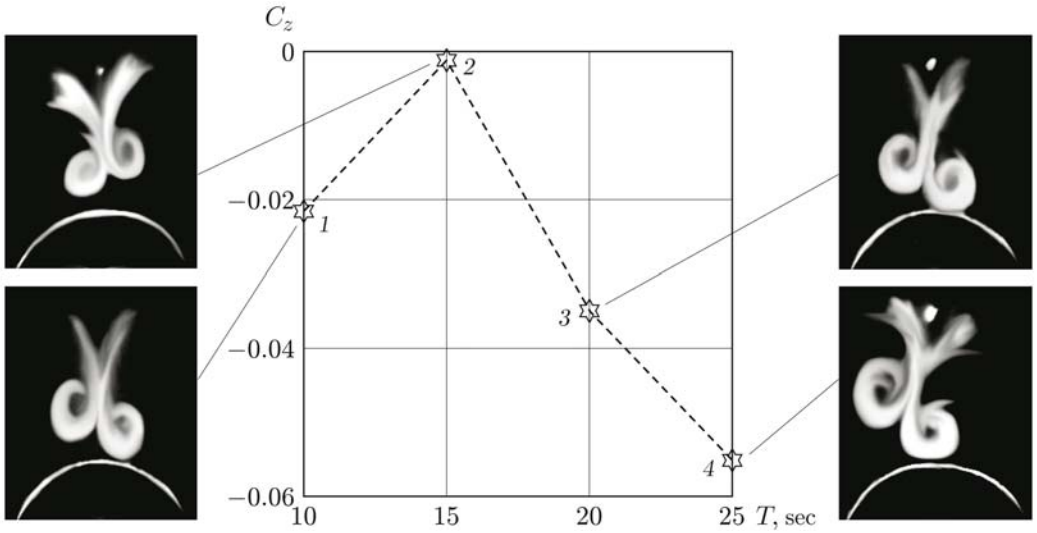

Fig. 7. Time evolution of the side load versus the left-hand discharge power and the corresponding vortex configurations (U_∞ = 10 m/sec and $\alpha = 17.5°$): W_2 = 0 (1), 11.2 (2), 44.8 (3), and 49.4 W (4).

The results of the experiment performed at an angle of attack $\alpha = 17.5°$ are illustrated in Fig. 7. The parameter varied in the experiment was the left-hand discharge power (the right-hand discharger was not used).

A comparison of the vortex patterns in Figs. 4 and 7, and also the corresponding dependences of the side force coefficient on the power supplied to the dischargers (see Figs. 6 and 7) shows that the behavior of the vortices is identical in two experiments. It should be noted that activation of a low-power discharge ($W = 11.2$ W) leads in both cases either to enhancement of asymmetry if the discharge is initiated on the side of the vortex located closer to the vortex surface (see Fig. 6) or to transformation of asymmetry to the opposite one if the discharge is initiated on the side of the vortex located farther from the model surface (see Fig. 7). The low-power discharge here

acts as a tripping device, which leads to a later flow separation on the side of this discharge and, therefore, makes the vortex approach the surface. With a further increase in power, the mechanism of the discharge action becomes different. In this case, the discharge can be considered as a geometric step. Its action on the flow is manifested in displacement of the streamlines and, therefore, displacement of the vortex farther from the model surface.

Conclusions. It was demonstrated in experiments that the use of an electric discharge in the vicinity of the cone tip aligned at an angle of attack is an effective method of flow control. The experiments were performed in wide ranges of subsonic flow parameters. It was possible both to transform an initially asymmetric flow to a symmetric form and to ensure directed asymmetry of the vortex configuration. Controlling the flow asymmetry, in turn, made it possible to control the side force direction. In addition, the dependence of the aerodynamic force on the action intensity was found to be monotonic. The use of a periodic spark discharge allowed the power necessary for effective flow control to be substantially reduced, as compared with the necessary arc discharge power. The data obtained show that the electric discharge can be used as an active element of control systems in promising flying vehicles. It was demonstrated that the discharge can be used not only to reduce the side loads, but also to generate controlling moments.

This work was supported by the Russian Foundation for Basic Research (Grant No. 09-08-00834-a), by the Integration Project No. 80-2009 of the Siberian Division of the Russian Academy of Sciences, and by the Analytical Department Targeted Program No. 2.1.2/3963 entitled "Development of higher school potential."

REFERENCES

1. A. W. Skow and D. J. Peake, "High angle of attack aerodynamics," AGARD Lecture Ser., No. 121, 10-1–10-22 (1982).
2. B. L. Hunt, "Asymmetric vortex forces and wakes on slender bodies," AIAA Paper No. 82-1336 (1982).
3. L. E. Ericsson and J. P. Reding, "Aerodynamic effects of asymmetric vortex shedding from slender bodies," AIAA Paper No. 85-1797 (1985).
4. P. J. Lamont, "Pressures around an inclined ogive cylinder with laminar, transitional, or turbulent separation," *AIAA J.*, **20**, No. 11, 1492–1499 (1982).
5. D. F. Fisher and B. R. Cobleigh, "Controlling forebody asymmetries in flight-experience with boundary layer transition strips," Tech. memorandum No. 4595, NASA, Washington (1994).
6. B. R. Cobleigh, "High-angle-of-attack yawing moment asymmetry of the X-31 aircraft from flight test," Report No. 186030, NASA, Washington (1994).
7. R. Kumar and P. R. Viswanath, "Nose bluntness for side control of circular cones at high incidence," AIAA Paper No. 2004-37 (2004).
8. C. A. Moskovits, R. M. Hall, and F. R. De Jarnette, "New device for controlling asymmetric flowfields on forebodies at large alpha," *J. Aircraft*, **28**, No. 7, 456–462 (1991).
9. J. E. Bernhardt and D. R. Williams, "Close-loop control of forebody flow asymmetry," *J. Aircraft*, **37**, No. 3, 491–498 (2000).
10. V. M. Fomin, A. A. Maslov, B. Yu. Zanin, et al., "Control of the vortex flow around a cone by an electric discharge," *Aeromekh. Gaz. Dinam.*, No. 4, 46–52 (2003).
11. V. M. Fomin, A. A. Maslov, A. A. Sidorenko, et al., "Control of the vortex flow around bodies of revolution by an electric discharge," *Dokl. Ross. Akad. Nauk*, **396**, No. 5, 1–4 (2004).
12. V. Shalaev, A. Fedorov, N. Malmuth, et al., "Plasma control of forebody nose symmetry breaking," AIAA Paper No. 2003-34 (2003).
13. V. I. Terekhov, N. I. Yarygina, and Ya. I. Smulsky, "Thermal and dynamic characteristics of the separated flow behind a flat rib with different angles of alignment toward the flow," *J. Appl. Mech. Tech. Phys.*, **48**, No. 1, 85–90 (2007).
14. R. M. Hall, "Forebody and missile side forces and the time analogy," AIAA Paper No. 87–0327 (1987).